approaches, especially in cases of malignant diseases. Although surgery is well accepted as a standard procedure in medicine there are still some problems left unsettled.

The technical difficulty of surgery is a common problem particularly for trainees, but even for experienced surgeons who have some technical limitations. Surgical procedures are difficult for regions deep in the body because the visual field for surgeons is limited, the number of surgical instruments which can be introduced is limited and the movements of these instruments are limited. One of the exemplary regions of this problem is the pelvic cavity, which includes surgery of rectal and prostate cancers.

Invasiveness is an inherent drawback to surgery, discouraging patients to undergo surgical treatment even when it is appropriate. It is true that surgery should be avoided when there are other less invasive alternatives.

Surgical robots such as the da Vinci system and the Zeus system are highly advanced medical instruments allowing for fine movements when appropriately manipulated by surgical experts. These systems are expected to solve some surgical problems such as invasiveness and the difficulty (4–8). Thus far, the systems have been able to solve some of the problems associated with surgery.

As for the invasiveness of surgery, endoscopic surgeries such as laparoscopy can be performed with robotic systems, utilizing smaller incisions than those of other standard open surgical approaches. The precise movements of surgeons are facilitated by robotic systems. However, laparoscopic procedures can be performed even without the robotic systems with the same amount of invasiveness.

Current robotic systems may also pose problems (4–8), such as the limited number of surgeons who can manipulate the system, which is usually one. Additional training for the specific manipulating methods of the systems is another problem, as well as introduction costs. Consequently, it is currently not clear what the benefits of these robotic systems are, especially when assessed from the patient side. Moreover, problems which even surgical experts suffer from have not been solved.

Flexible endoscopes have been developed to cope with the problems of accessing regions through narrow tracts such as the esophagus and the tracheobronchial tree. Even in these regions flexible endoscopes can perform surgical procedures similar to standard surgery. Therefore, endoscopes are naturally considered functional even in other cavities such as the abdomen and pelvic cavities.

It would be easier and more functional to perform an operation using several endoscopic instruments introduced through the end of one endoscope, rather than conducting resection using only one endoscopic instrument introduced into one endoscope, as done in standard endoscopic procedures. The simplest model for this concept is the flexible endoscopic surgical system we developed and examined within these trials.

We assumed that there would be several problems with the flexible endoscopic surgical system when used clinically as it is merely a conceptual model to confirm its feasibility of use. However, despite those problems, the system was able to perform surgical resection. In addition, the problems encountered within the first experiment were inherent in all technical procedures.

Of interest, these problems showed us that, when indicated for resecting procedures, the flexible endoscopic surgical system is easier to manipulate by surgeons and not by endoscopists despite its endoscopic appearances.

The images of the inner endoscopes were not satisfactory because a CCD was not used in these endoscopes. Consequently, resecting procedures were monitored by images from the outer endoscope which contained the CCD. In this situation, the operator had to control the inner endoscope via observations on the monitor of the outer endoscope. This is different from standard endoscopic procedures in which images are observed on the monitor of the endoscope which the operator is controlling.

In general, it is not easy for trainees to understand appropriate surgical procedures, i.e. where to cut and where to stabilize. Verbal communication during operation is important to facilitate appropriate assistance, which was not adequately utilized in the first series. These issues are to be learned through years of experience and cannot be achieved instantly.

As mentioned above, the difference between the two experiments may reveal that for these flexible endoscopes, surgical experience is an important factor, when the system is indicated for surgical procedures. The limitation of the inner endoscopes, not having CCD may have emphasized this issue. Consequently, the next system is to consist of two inner endoscopes with a CCD for each. This would allow the operators to control the inner endoscopes in such a manner as used for standard gastrointestinal endoscopic procedures.

Furthermore, we think that there should be two styles of design for future flexible endoscopic surgical systems; one with increased surgical maneuverability designed particularly for the techniques of surgeons, the other preserving flexible endoscopic maneuverability for endoscopists. Although it has not been decided yet which design is more appropriate for a future surgical system, endoscopists may be able to become accustomed to the flexible endoscopic surgical system with surgical maneuverability when the system is popularized.

In addition to the merits mentioned above, flexible endoscopic materials can theoretically be made compatible with X-ray systems such as fluoroscopes and computed tomography (CT) systems, exemplified by such procedures as X-ray guided bronchoscopy. In the future, the materials used for flexible endoscopic constructions are expected to acquire compatibility with the magnetic fields of magnetic resonance imaging (MRI) systems.

As mentioned before, limitations in visualization pose surgical problems even for experienced surgeons. This may only partially be solved by the subjective ability of surgeons to presume the identity of invisible objects using their tactile sense and their intuition. Actually, the compatibility with imaging systems was one of the important requirements for the design of the flexible endoscopic surgical system,

allowing visibility of anatomical information invisible to the surgeon's eyes.

In order to make one more step towards the future for less invasive and more effective medical treatments, we believe that future surgical systems should acquire the accessibility to narrow regions located deep inside the body together with the compatibility of imaging systems such as CT and MRI. Thus, from the flexible nature and structural characteristics of a non-jointed, smooth outer sheath, we selected the flexible endoscope as the conceptual basis of development for our system. It is the combination of these and the aforementioned aspects that allows for minimization in invasiveness, through the use of pre-existing natural structures and tracts for lesion access to deep regions, and with the presence of multiple interchangeable inner-scopes, an increase in distal tip functionality at the surgical site. Although there are several factors still to discuss and develop, the concept of the flexible endoscopic surgical system is considered an appropriate development for a future surgical robotic system with this current system being a successful step towards that furture.

Acknowledgments

This study was supported by a Grant-in-Aid for Research on Medical Devices for Analyzing, Supporting and Substituting the Function of Human Body from the Ministry of Health, Labour and Welfare.

References

1. Kobayashi T, Gotohda T, Tamakawa K, Ueda H, Kakizoe T. Magnetic anchor for more effective endoscopic mucosal resection. *Jpn J clin Oncol* 2004;34:118–23.
2. Gotoda T, Yanagisawa A, Sasako M, Ono H, Nakanishi Y, Shimoda T, et al. Incidence of lymph node metastasis from early gastric cancer: estimation with a large number of cases at two large centers. *Gastric Cancer* 2000;3:219–25.
3. Gotoda T, Kondo H, Ono H, Saito Y, Yamaguchi H, Saito D, et al. A new endoscopic mucosal resection procedure using an insulation-tipped electrosurgical knife for rectal flat lesions: report of two cases. *Gastrointest Endosc* 1999;50:560–3.
4. D'Anniballe A, Fiscon V, Trevisan P, Pozzobon M, Gianfreda V, Sovernigo G, et al. The da Vinci robot in right adrenalectomy: considerations on technique. *Surg Laparosc Endosc Percutan Tech* 2004;14:38–41.
5. Schiff J, Li PS, Goldstein M. Robotic microsurgical vasovasostomy and vasoepididymostomy: a prospective randomized study in a rat model. *J Urol* 2004;171:1720–5.
6. Ruurda JP, Broeders IA, Simmermacher RP, Borel Rinkes IH, Van Vroonhoven TJ, Theo JM. Feasibility of robot-assisted laparoscopic surgery: an evaluation of 35 robot-assisted laparoscopic cholesystectomies. *Surg Laparosc Endosc Percutan Tech* 2002;12:41–5.
7. Falk V, Diegler A, Walther T, Autschbach R, Mohr FW. Developments in robotic cardiac surgery. *Curr Opin Cardiol* 2000;15:378–87.
8. Hollands CM, Dixey LN. Applications of robotic surgery in pediatric patients. *Surg Laparosc Endosc Percutan Tech* 2002;12:71–6.

^{11}C-Acetate Positron Emission Tomography Imaging for Lung Adenocarcinoma 1 to 3 cm in Size With Ground-Glass Opacity Images on Computed Tomography

Hiroaki Nomori, MD, PhD, Noboru Kosaka, MD, PhD, Kenichi Watanabe, MD, Takashi Ohtsuka, MD, Tsuguo Naruke, MD, PhD, Toshiaki Kobayashi, MD, PhD, and Kimiichi Uno, MD, PhD

Department of Thoracic Surgery, Graduate School of Medical and Pharmaceutical Sciences, Kumamoto University; Department of Thoracic Surgery, Saiseikai Central Hospital; Development in Assistive Diagnostic Technology, National Cancer Center Hospital, and Nishidai Clinic, Tokyo, Japan

Background. Positron-emission tomography (PET) with ^{18}F-fluorodeoxy-glucose (FDG) frequently gives false-negative results for well-differentiated adenocarcinomas of the lung, especially, those with ground-glass opacity images. Recently, PET with ^{11}C-acetate (AC) has been reported to detect slow-growing tumors that have failed to be identified by FDG-PET, such as well-differentiated hepatocellular carcinomas and prostate cancers. To determine the usefulness of AC-PET in detecting well-differentiated adenocarcinomas of the lung, we performed both AC-PET and FDG-PET on pulmonary nodules with ground-glass opacity images on computed tomography (CT).

Methods. Fifty-four pulmonary nodules 1 to 3 cm in size, which showed ground-glass opacity images over their whole or peripheral area on CT, were examined by both AC-PET and FDG-PET.

Results. Thirty-seven nodules were adenocarcinoma of the lung, while 17 were inflammatory. Of the 37 adenocarcinomas, 19 (51%) were positively identified by AC-PET and 14 (38%) by FDG-PET. Of the 23 adenocarcinomas which were not identified by FDG-PET, 8 (35%) were positively identified by AC-PET; all were well-differentiated adenocarcinomas. Of the 17 inflammatory nodules, 8 were chronic and 9 were acute ones. While none of the 8 chronic inflammatory nodules were identified by either technique, 9 acute ones showed a variety of the results with AC- and FDG-PET.

Conclusions. AC-PET detected approximately one third of well-differentiated adenocarcinomas of the lung which were not identified by FDG-PET. AC-PET could be useful to diagnose pulmonary nodules with ground-glass opacity images which were not identified by FDG-PET.

(Ann Thorac Surg 2005;80:2020–5)

Recent advances in positron emission tomography (PET) with ^{18}F-fluorodeoxy-glucose (FDG) have contributed significantly to the ability to differentiate between benign and malignant pulmonary nodules. However, FDG-PET sometimes gives false-negative results, particularly for low-grade malignant tumors, such as bronchioloalveolar carcinoma and carcinoid, owing to their low glucose metabolism [1–4]. We previously reported that while FDG-PET did not produce false-negative results for squamous cell, large cell, or small cell carcinomas, 60% of well-differentiated adenocarcinomas 1 to 3 cm in size failed to be identified by FDG-PET [2]. Therefore, other PET tracers should be used for imaging suspected well-differentiated adenocarcinoma of the lung.

Radio-labeled acetate has long been used for the measuring lipid and cholesterol synthesis in biochemistry [5, 6]. Clinically, ^{11}C-acetate (AC) has been widely used as a PET tracer for evaluating myocardial oxidative metabolism [7, 8]. Recently, AC has also been reported to be a useful PET tracer in detecting slow-growing tumors which have failed to be identified by FDG-PET, such as well-differentiated hepatocellular carcinomas and prostate cancers [9, 10]. Higashi and colleagues [11] have also reported a patient with bronchioloalveolar carcinoma that was positively identified by AC-PET but not by FDG-PET. In the present study, to evaluate the effectiveness of AC-PET in detecting well-differentiated adenocarcinomas of the lung, we performed both AC-PET and FDG-PET on 54 small pulmonary nodules suspected of being adenocarcinomas based on computed tomography (CT) findings.

Material and Methods

Patients and Tumor Tissues

The pulmonary nodules of 1 to 3 cm in size, which were suspected of being well-differentiated adenocarcinoma of

Accepted for publication June 3, 2005.

Address correspondence to Dr Nomori, Department of Thoracic Surgery, Graduate School of Medical and Pharmaceutical Sciences, Kumamoto University, 1-1-1 Honjo, Kumamoto 860-8556, Japan; e-mail address: hnomori@qk9.so-net.ne.jp.

Published by Elsevier Inc

0003-4975/05/$30.00
doi:10.1016/j.athoracsur.2005.06.003

Table 1. FDG-PET and Acetate-PET Findings in Adenocarcinomas and Inflammatory Nodules

Procedures	Adenocarcinoma	Inflammation	Total
FDG-PET			
Positive	14	5	19
Negative	23	12	35
Acetate-PET			
Positive	19	5	24
Negative	18	12	30
Total	37	17	54

FDG = fluorodeoxyglucose; PET = positron emission tomography.

the lung owing to the presence of ground-glass opacity images over their whole or peripheral area on CT [12–15], were performed of both FDG-PET and AC-PET to evaluate the usefulness of AC-PET. The study was approved by the Ethical Committee of Saiseikai Central Hospital in December 2003. The reason why we excluded the nodules less than 1 cm was that the spatial resolution of the current generation of PET scanners is 0.7 to 0.8 cm, making it difficult to image pulmonary nodules of less than 1 cm [2]. Between January 2004 and April 2005, 54 pulmonary nodules with ground-glass opacity images in 50 patients were enrolled. Three patients have a few nodules, which were located in the different lobes of each other in each patient. During the same period, 85 pulmonary nodules up to 3 cm with solid images in 82 patients were examined only by FDG-PET. Of the 54 nodules, 37 were adenocarcinoma of the lung and 17 were inflammatory. The diagnosis was confirmed histologically after surgical resection in all 37 of the adenocarcinomas, 8 of the nodules with chronic inflammation, 2 with active tuberculosis, and 1 with active nonspecific inflammation. The remaining 6 nodules were clinically diagnosed as acute inflammatory nodules because of natural reduction on follow-up CT. The lung adenocarcinomas were classified as well-, moderately, and poorly differentiated. The percentage area showing ground-glass opacity on CT was graded as more than 90%, 30% to 90%, or less than 30%.

Positron Emission Tomography Scanning

Positron emission tomography scanning was performed at Nishidai Clinic, Tokyo, Japan. Patients were instructed to fast for at least 4 hours before PET scanning. After a written informed consent had been obtained, AC- and FDG-PET were performed on the same day within 2 weeks of CT scanning. The AC-PET was performed before FDG-PET. The dose of ^{11}C-AC administered was 125 μCi/kg (4.6 MBq/kg). The PET imaging was performed approximately 10 minutes after the administration of ^{11}C-AC using a PosiCam.HZL mPower scanner (Positron, Houston, Texas).

The ^{18}F-FDG was administered approximately 30 minutes after AC-PET imaging was completed, ensuring that a gap of at least 120 minutes was left between the administration of ^{11}C-AC and that of ^{18}F-FDG, namely, more than 6 decay half-lives of ^{11}C (20 minutes). The dose of ^{18}F-FDG was 125 μCi/kg (4.6 MBq/kg) for nondiabetic patients and 150 μCi/kg (5.6 MBq/kg) for diabetic patients, as reported previously [2–4]. The FDG-PET imaging was performed approximately 45 minutes after the administration of FDG.

No attenuation-corrected emission scans were initially obtained in two-dimensional, high-sensitivity mode for 4 minutes per bed position, and taken from the vertical skull through to the mid thighs. Immediately thereafter, a two-bed-position, attenuation-corrected examination was performed, with 6 minutes for the emission sequence and 6 minutes for the transmission sequence at each bed position. The images were reconstructed by the emission scans and the preinjection transmission scans in a 128 × 128 matrix by using ordered subset expectation maximization corresponding to a pixel size of 4 × 4 mm, with section spacing of 2.56 mm.

Positron Emission Tomography Data Analysis

Images were reviewed by two observers (N.K. and K.U.) who were unaware of the patients' clinical details. A consensus was reached if there was any difference of opinion. PET images were evaluated by visual assessment, namely, lesions showing similar or greater AC or FDG uptake than the mediastinal blood pool were diagnosed as positive for tumor. The AC and FDG uptakes of the positive nodules were measured on the basis of the contrast ratio, as reported previously [2–4]. Briefly, regions of interest were chosen in the nodules and contralateral lung. The highest standard uptake value in the tumor regions of interest (T) and the contralateral normal lung regions of interest (N) were then measured and the contrast ratio was calculated as $(T - N)/(T + N)$ in each nodule as an index of AC and FDG uptake.

Evaluation by Receiver Operating Characteristics Curve

Usefulness of detecting well-differentiated adenocarcinoma by FDG- and AC-PET was evaluated by receiver operating characteristics (ROC) curves. The contrast ratio values of 27 well-differentiated adenocarcinomas and 27 other lesions (10 moderately or poorly differentiated adenocarcinomas and 17 inflammatory nodules) of FDG-PET and AC-PET were compared on ROC curve by using SPSS software (SPSS, Chicago, Illinois).

Statistical Analysis

Positive PET findings with malignancy and benign nodules were defined as true positive (TP) and false positive

Table 2. Summary of Results of FDG-PET and Acetate-PET

Variables	FDG-PET	Acetate-PET
Sensitivity	0.38	0.51
Specificity	0.71	0.71
Positive predictive value	0.74	0.79
Negative predictive value	0.34	0.40
Accuracy	0.48	0.57

FDG = fluorodeoxyglucose; PET = positron emission tomography.

Table 3. Correlation Between Histologic Grade of Differentiation of Adenocarcinomas and PET Findings

PET Imaging Findings	Histologic Differentiation			
	WD	MD	PD	Total
Acetate positive, FDG positive	5	5	1	11
Acetate positive, FDG negative	8	0	0	8
Acetate negative, FDG positive	0	3	0	3
Acetate negative, FDG negative	14	1	0	15
Total	27	9	1	37

FDG = fluorodeoxyglucose; MD = moderately differentiated; PD = poorly differentiated; PET = positron emission tomography; WD = well differentiated.

(FP), respectively. Negative PET findings with malignancy and benign nodules defined as false negative (FN) and true negative (TN), respectively. The diagnostic values of PET scanning were assessed by calculating sensitivity and specificity. Sensitivity was calculated as TP/TP + FN, specificity as TN/TN + FP, positive predictive value as TP/TP + FP, negative predictive value as TN/FN + TN, and accuracy as TP + TN/total. All data were analyzed for significance by using the two-tailed Student *t* test. Values of *p* less than 0.05 were accepted as significance. All values in the text and tables are given as mean ± SD.

Results

Table 1 shows the PET findings of adenocarcinomas and inflammatory nodules. Mean sizes were 2.1 ± 0.7 cm for the 37 adenocarcinomas and 1.7 ± 0.8 cm for the 17 inflammatory nodules; this difference was not significant. Of the 37 adenocarcinomas, 19 were positively identified by AC-PET and 14 by FDG-PET. The sensitivity, specificity, positive predictive value, negative predictive value, and accuracy were not significant different between the FDG-PET and AC-PET (Table 2). Eleven adenocarcinomas were positively identified by both AC- and FDG-PET, 8 were positively identified by AC-PET but not by FDG-PET, 3 were positively identified by FDG-PET but not by AC-PET, and the remaining 15 failed to be identified by either technique (Table 3). Of the 17 inflammatory nodules, 3 were positively identified by both AC-PET and FDG-PET, 2 were positively identified by AC-PET but not by FDG-PET, 2 were positively identified by FDG-PET but not by AC-PET, and the remaining 10 were negative by either technique (Table 4).

Table 4. FDG-PET and Acetate-PET Findings in Inflammatory Nodules

PET Imaging Findings	Chronic Inflammation	Acute Inflammation	Total
Acetate positive, FDG positive	0	3	3
Acetate positive, FDG negative	0	2	2
Acetate negative, FDG positive	0	2	2
Acetate negative, FDG negative	8	2	10
Total	8	9	17

FDG = fluorodeoxyglucose; PET = positron emission tomography.

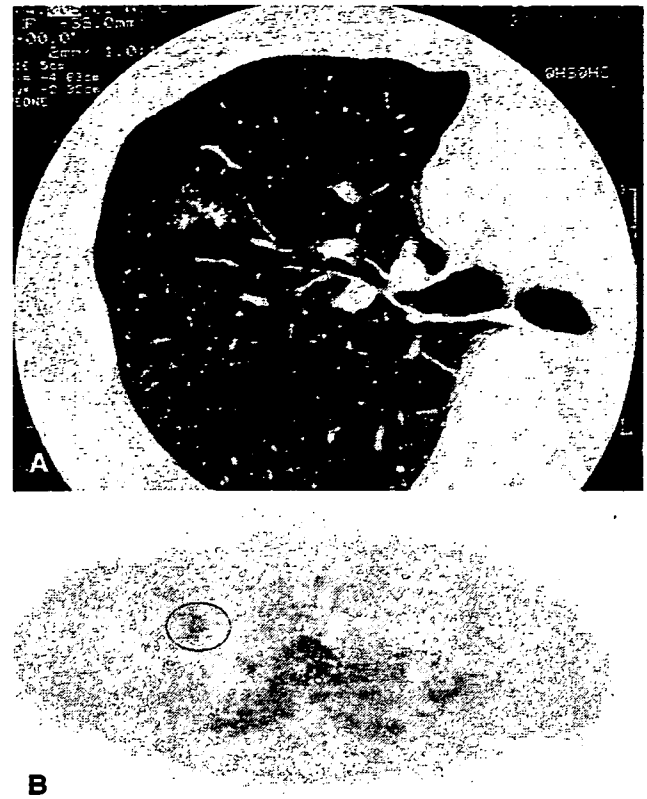

Fig 1. (A) Computed tomography findings of well-differentiated adenocarcinoma with ground-glass opacity findings. (B) Acetate-positron emission tomography showed positive at the tumor (encircled).

Table 3 also shows the correlation between the histologic grade of differentiation and the PET findings in the 37 adenocarcinomas. The histologic grades were well differentiated in 27 adenocarcinomas, moderately differentiated in 9, and poorly differentiated in 1. Of the 23 adenocarcinomas which failed to be identified by FDG-PET, 8 (36%) were positively identified by AC-PET, all of which were well-differentiated ones (Fig 1), whereas none of moderately or poorly differentiated adenocarcinomas were positive with AC-PET and negative with FDG-PET. Well-differentiated adenocarcinomas were more frequently positive with AC-PET and negative with FDG-PET than moderately or poorly differentiated adenocarcinomas ($p = 0.051$). Of the 15 adenocarcinomas which failed to be identified by either technique, 14 (93%) were well-differentiated ones and the remaining 1 (7%) was moderately differentiated. Well-differentiated ade-

Table 5. Correlation Between Percent of GGO Area and Histologic Grade of Differentiation of Adenocarcinomas

	Histologic Differentiation			
Percent of GGO Area	WD	MD	PD	Total
≥90%	19[a]	1	0	20
30%–90%	5	0	0	5
<30%	3	8	1	12
Total	27	9	1	37

[a] Well-differentiated adenocarcinoma showed more than 90% of GGO area more frequently than moderately or poorly differentiated ($p < 0.01$).

GGO = ground-glass opacity; MD = moderately differentiated; PD = poorly differentiated; WD = well-differentiated.

nocarcinomas were more frequently negative with both AC-PET and FDG-PET than moderately or poorly differentiated adenocarcinomas ($p = 0.03$).

Both AC and FDG uptake of these adenocarcinomas were usually weak by visual assessment. In the 19 adenocarcinomas detected by AC-PET, the mean values of contrast ratio and standard uptake value were 0.3 ± 0.1 (range, 0.25 to 0.42) and 2.3 ± 0.7 (range, 1.1 to 3.4), respectively. In the 13 adenocarcinomas detected by FDG-PET, the mean values of contrast ratio and standard uptake value was 0.4 ± 0.2 (range, 0.25 to 0.8) and 3.2 ± 1.8 (range, 1.0 to 7.4), respectively.

Table 4 shows the FDG- and AC-PET findings in the 17 inflammatory nodules. While none of the 8 nodules with chronic inflammation were detected by either AC- or FDG-PET, 9 nodules with acute inflammation showed a variety of the results.

Table 5 shows the correlation between the percentage area of ground-glass opacity and the histologic grade of differentiation in the 37 adenocarcinomas. Ground-glass opacity was apparent over more than 90% of the tumor area in 20 adenocarcinomas, 30% to 90% in 5, and less than 30% in the remaining 12. Well-differentiated adenocarcinomas showed more than 90% of ground-glass opacity area more frequently than moderately or poorly differentiated ones ($p < 0.01$).

Figure 2 shows the ROC curves of FDG- and AC-PET for detecting 27 well-differentiated adenocarcinoma in the 54 nodules with ground-glass opacity images. The ROC curve of AC-PET was superior to that of FDG-PET. The areas under the curve were 0.573 in AC-PET and 0.318 in FDG-PET. The 95% confidential limits showed little overlap between the AC-PET (range, 0.414 to 0.733) and FDG-PET (range, 0.174 to 0.461).

The tumor size did not show any correlation not only with contrast ratio values and standard uptake value of FDG-PET ($r = 0.31$ and $r = 0.38$, respectively) but also with contrast ratio values and standard uptake value of AC-PET ($r = 0.1$ and $r = 0.08$, respectively).

Comment

While a criterion for diagnosing pulmonary malignancy with FDG-PET has frequently used the standard uptake value with a cut-off value of 2.5 [16], it has been reported that several factors can affect the standard uptake value, such as the body size [17], blood glucose concentration [18], time after injection [19], and lesion size [20]. Actually, the mean standard uptake value of malignant pulmonary nodules has been reported to be various, ranging from 5.5 to 10.1 [21–24]. We previously compared the results of standard uptake value, contrast ratio with contralateral lung, and contrast ratio with cerebellum for diagnosing pulmonary nodules with faintly positive FDG uptake by visual estimation, and reported the cut-off value of 0.4 by the contrast ratio with contralateral lung to show the highest sensitivity, while the standard uptake value of 2.5 showing the sensitivity of 0 [25]. We therefore used the contrast ratio with contralateral lung in the present study. Both AC and FDG uptake in the present adenocarcinomas were usually weak. The mean contrast ratio values of AC and FDG uptake of the positive adenocarcinomas in the present study were 0.3 ± 0.1 and 0.4 ± 0.2, respectively, both of which were near the cut-off value for diagnosing lung cancers. It could be due to that most of adenocarcinomas in the present study were well-differentiated ones, which were known to show weak or negative PET imaging frequently [1–4].

Well-differentiated adenocarcinomas of the lung have been reported to show a high false-negative identification rate on FDG-PET because of their low glucose metabolism and low tumor cell density [1–4]. These observations were confirmed by the present study in which 22 of the 27 well-differentiated adenocarcinomas (81%) failed to be detected by FDG-PET (as shown in Table 3). While ^{11}C-AC has been reported to be a useful PET tracer for slow-growing tumors, such as well-

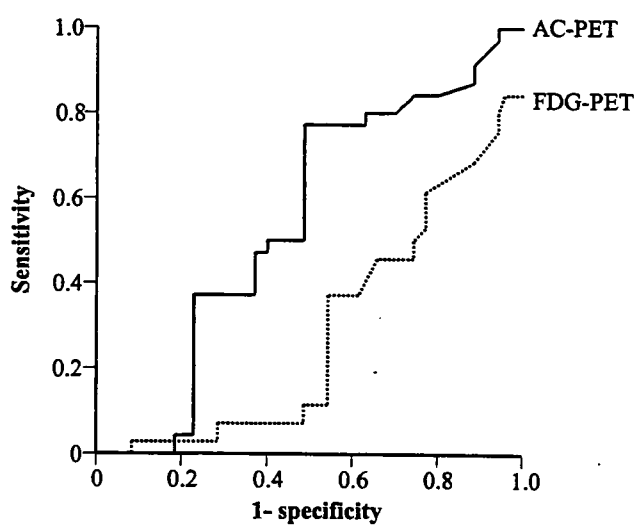

Fig 2. The receiver operating characteristic curve of ^{11}C-acetate positron emission tomography (AC-PET; solid line) *and ^{18}F-fluorodeoxy-glucose PET* (FDG-PET; dotted line) *for detecting 27 well-differentiated adenocarcinoma in the 54 nodules with ground-glass opacity images. The areas under the curve were 0.573 in AC-PET and 0.318 in FDG-PET. The 95% confidence limits were from 0.414 to 0.733 in AC-PET and from 0.174 to 0.461 in FDG-PET.*

differentiated hepatocellular carcinomas and prostate cancers [9, 10], the present study showed that there was no significant difference in sensitivity between AC-PET and FDG-PET with respect to adenocarcinomas of the lung. However, of the 23 adenocarcinomas not identified by FDG-PET, 8 (35%) were positively identified by AC-PET; all of these were well-differentiated adenocarcinomas. Therefore, AC-PET was able to detect approximately one third of well-differentiated adenocarcinomas that were not detected by FDG-PET.

Ho and Yeung [9] reported that while well-differentiated hepatocellular carcinomas had a high AC uptake and a low FDG uptake, poorly differentiated ones had a low AC uptake and a high FDG uptake. Thus, hepatocellular carcinomas could be detected with 100% sensitivity by using both AC-PET and FDG-PET [9]. In contrast, Oyama and colleagues [10] reported that all 22 of their patients' prostate cancers were positively identified by AC-PET. However, the present study showed that 15 of the 37 lung adenocarcinomas (41%) could not be detected by either AC- or FDG-PET, and 14 of these 15 (93%) were well-differentiated adenocarcinomas. There are several reasons why well-differentiated adenocarcinomas of the lung may frequently go undetected by both AC-PET and FDG-PET. Firstly, well-differentiated lung adenocarcinomas may accumulate AC and FDG to only a limited extent due to lower metabolism of these substances compared with hepatocellular carcinomas and prostate cancers. Secondly, because well-differentiated adenocarcinomas frequently show ground-glass opacity images over a large area (as shown in Table 5), the density of the tumor cells is low compared with moderately or poorly differentiated ones, and that could be false-negative results of PET imaging, regardless of the degree of tracer uptake by the tumor cells. Thirdly, because all the adenocarcinomas in the present study were less than 3 cm in size, their AC or FDG uptake may have been below the limit of detection compared with larger ones.

The tracer ^{11}C-acetate has been widely used as a PET tracer for the evaluation of myocardial oxidative mechanism [7, 8]. The mechanism underlying AC uptake in tumor cells, although as yet unknown, is thought to be different from that involved in myocardial uptake. In an in vitro study using several cancer cell lines, Yoshimoto and colleagues [25] suggested that AC is preferentially metabolized to membrane lipids in tumor cells and that AC uptake by tumor cells reflects their growth activity as measured by enhanced membrane synthesis. On the other hand, Ho and Yeung [9] reported that the AC uptake of hepatocellular carcinomas showed negative correlation with their malignant potential. In the present study, while some of the well-differentiated adenocarcinomas were positively identified by AC-PET but not by FDG-PET, some of the well-, moderately, and poorly differentiated adenocarcinomas were positively identified by both technique. Based on our present data, we hypothesize the following: (1) Whereas FDG may be accumulated by aggressive lung cancer cells [26, 27], AC might be accumulated by slow-growing ones, as in the case with hepatocellular carcinomas and prostate cancers [9, 10]. (2) Whereas most lung cancers can accumulate both AC and FDG because of containing tumor cells having different growth activity, some well-differentiated adenocarcinomas, which only contain less aggressive tumor cells, may be able to accumulate only AC.

Both chronic and acute inflammatory pulmonary nodules are well known to show ground-glass opacity images on occasions. In the present study, while all of the chronic inflammatory nodules were negative by both AC-PET and FDG-PET, the acute ones showed a variety of the results. That could be because the acute inflammatory nodules have a variety of percentages of inflammatory cells having different grades of metabolic activity, such as leukocytes, lymphocytes, and macrophages, according to the phase of inflammation.

Positron emission tomography with AC could be useful for some of pulmonary nodules with ground-glass opacity images that could not be identified by FDG-PET. In the present study, most of the nodules studied were well-differentiated adenocarcinomas because the nodules were selected on the basis of the presence of ground-glass opacity images. Therefore, AC-PET needs to be studied in other histologic types of lung cancer to clarify its usefulness in detecting lung cancers in general.

This work was supported in part by a Grant-in-Aid from the Ministry of Health, Labor and Welfare of Japan.

References

1. Higashi K, Ueda Y, Seki H, et al. Fluorine-18-FDG PET imaging is negative in bronchioloalveolar carcinoma. J Nucl Med 1998;39:1016–20.
2. Nomori H, Watanabe K, Ohtsuka T, Naruke T, Suemasu K, Uno K. Evaluation of F-18 fluorodeoxyglucose (FDG) PET scanning for pulmonary nodules less than 3 cm in diameter, with special reference to the CT images. Lung Cancer 2004;45:19–27.
3. Nomori H, Watanabe K, Ohtsuka T, et al. Fluorine 18-tagged fluorodeoxyglucose positron emission tomographic scanning to predict lymph node metastasis, invasiveness, or both, in clinical T1N0M0 lung adenocarcinoma. J Thorac Cardiovasc Surg 2004;128:396–401.
4. Nomori H, Watanabe K, Ohtsuka T, Naruke T, Suemasu K, Uno K. Visual and semiquantitative analyses from F-18 fluorodeoxyglucose (FDG) PET scanning in pulmonary nodules 1 to 3 cm in size. Ann Thorac Surg 2005;79:984–8.
5. Howard BV. Acetate as a carbon source for lipid synthesis in cultured cells. Biochim Biophys Acta 1977;488:145–51.
6. Long VJW. Incorporation of 1-11C-acetate into the lipids of isolated epidermal cells. Br J Dermatol 1976;94:243–52.
7. Brown M, Marshall DR, Sobel BE, Bergmann SR. Delineation of myocardial oxygen utilization with carbon-11-labeled acetate. Circulation 1987;76:687–96.
8. Lear JL. Relationship between myocardial clearance rates of carbon-11-acetate-deribed radiolabel and oxidative metabolism: physiologic basis and clinical significance. J Nucl Med 1991;32:1957–60.
9. Ho C, Yeung DW. C-11 acetate PET imaging in hepatocellular carcinoma and other liver masses. J Nucl Med 2003;44:213–21.
10. Oyama N, Akino H, Kanamaru H, et al. 11C-acetate PET imaging of prostate cancer. J Nucl Med 2002;43:181–6.

11. Higashi K, Ueda Y, Matsunari I, et al. 11C-acetate PET imaging of lung cancer: comparison with 18F-FDG and 99mTc-MIBI SPET. Eur J Nucl Med Mol Imaging 2004; 31:13–21.
12. Aoki T, Nakata H, Watanabe H, et al. Evolution of peripheral lung adenocarcinomas: CT findings correlated with histology and tumor doubling time. Am J Roentgenol 2000;174: 763–8.
13. Nakata M, Saeki H, Takata I, et al. Focal ground-glass opacity detected by low-dose helical CT. Chest 2002;121: 1464–7.
14. Nomori H, Ohtsuka T, Naruke T, Suemasu K. Differentiating between atypical adenomatous hyperplasia and bronchioloalveolar carcinoma using the computed tomography number histogram. Ann Thorac Surg 2003;76:867–71.
15. Nomori H, Ohtsuka T, Naruke T, Suemasu K. Histogram analysis of computed tomography numbers of clinical T1N0M0 lung adenocarcinoma, with special reference to lymph node metastasis and tumor invasiveness. J Thorac Cardiovasc Surg 2003;126:1584–9.
16. Langen KJ, Braun U, Rota Kops E, et al. The influence of plasma glucose levels of fluorine-18-fluorodeoxyglucose uptake in bronchial carcinomas. J Nucl Med 1993;34:355–9.
17. Kim CK, Gupta NC, Chandramouli B, Alavi A. Standarized uptake values of FDG: body surface area correction is preferable to body weight correction. J Nucl Med 1994;35: 164–7.
18. Lindholm P, Minn H, Leskinen-Kallio S, Bergman J, Ruotsalainen U, Joensuu H. Influence of the blood glucose concentration on FDG uptake in cancer—a PET study. J Nucl Med 1993;34:1–6.
19. Hamberg LM, Hunter GI, Alpert NM, Choi NC, Babich JW, Fischman AJ. The dose uptake ratio as an index of glucose metabolixm: useful parameter or oversimplification? J Nucl Med 1994;35:1308–12.
20. Menda Y, Bushnell DL, Madsen MT, McLaughlin K, Kahn D, Kernstine KH. Evaluation of various corrections to the standardized uptake value for diagnosis of pulmonary malignancy. Nucl Med Commun 2001;22:1077–81.
21. Dewan NA, Gupta NC, Redepenning LS, et al. Diagnostic efficacy of PET-FDG imaging in solitary pulmonary nodules. Chest 1993;104:997–1002.
22. Gupta NC, Maloof J, Gunel E. Probability of malignancy in solitary pulmonary nodules using fluorine-18-FDG and PET. J Nucl Med 1996;37:943–8.
23. Imdahl A, Jenkner S, Brink I, et al. Validation of FDG positron emission tomography for differentiation of unknown pulmonary lesions. Eur J Cardiothorac Surg 2001;20: 324–9.
24. Lowe VJ, Fletcher JW, Gobar L, et al. Prospective investigation of positron emission tomography in lung nodules. J Clin Oncol 1998;16:1075–84.
25. Yoshimoto M, Waki A, Yonekura Y, et al. Characterization of acetate metabolism in tumor cells in relation to cell proliferation: acetate metabolism in tumor cells. Nucl Med Biol 2001;28:117–22.
26. Higashi K, Ueda Y, Yagishita M, et al. FDG PET measurement of the proliferative potential on non-small cell lung cancer. J Nucl Med 2000;41:85–92.
27. Vesselle H, Schmidt RA, Pugsley JM, et al. Lung cancer proliferation correlates with [F-18] fluorodeoxyglucose uptake by positron emission tomography. Clin Cancer Res 2000;6:3837–44.

Recent Advances in Radiology for the Diagnosis of Gastric Carcinoma

Gen Iinuma[1], Hideto Tomimatsu[1], Yukio Muramatsu[1], Noriyuki Moriyama[1], Toshiaki Kobayashi[2], Hiroshi Saito[2], Tetsuo Maeda[3], Kunihisa Miyakawa[3], Fumihiko Wakao[3], Mitsuo Satake[3], and Yasuaki Arai[3]

Introduction

Radiographic diagnosis of gastric carcinoma [1] was first introduced in the 1960s in Japan, which led the world in the early diagnosis of gastric carcinoma by double-contrast method using film-screen systems (FSS) [2,3]. Qualitative diagnostics, including diagnosis of the depth of tumor invasion, were explored thoroughly in the 1970s, and it could be claimed that the radiographic diagnosis of gastric carcinoma was completely established by the beginning of the 1980s [4]. Gastric radiography has now become a standard examination modality in the screening and preoperative staging of gastric carcinoma and is widely used across the globe. The mortality rate from gastric carcinoma is especially high in Japan, and gastric radiography has made a substantial contribution to the detection of gastric carcinoma in mass screening. With recent advances in endoscopic techniques, the primary role in the diagnosis of gastric carcinoma, including its early diagnosis, has been inherited by endoscopy, but it is also a fact that radiography is still widely used in clinical diagnosis in screening and preoperative staging [5]. The demand for computerization of medical information grew in the 1980s, and against a background of advances in image engineering, the digitalization of medical images has proceeded apace [6,7]. In gastric radiography, too, digitalization via digital radiography (DR) using high-resolution charge-coupled device (CCD) cameras (CCD-DR) has been established and disseminated rapidly, and we also have reported its usefulness in the diagnosis of gastric carcinoma [8]. Meanwhile, a recent major development in the field of radiology has been the emergence of multidetector row computed tomography (CT) (MDCT) [9]. With the advent of MDCT in the second half of the 1990s, CT has achieved increased efficiencies and improved image quality in a revolutionary scanning modality [10]. In the preoperative staging of gastric carcinoma, it is now possible to accurately evaluate local inva-

[1] Cancer Screening Division, Research Center for Cancer Prevention and Screening, [2] Cancer Screening Technology Division, Research Center for Cancer Prevention and Screening, [3] Diagnostic Radiology Division, National Cancer Center Hospital, National Cancer Center, 5-1-1 Tsukiji, Chuo-ku, Tokyo 104-0045, Japan
e-mail: giinuma@gan2.ncc.go.jp

sion and small metastases, and three-dimensional (3D) MDCT imaging (MDCT gastrography) has arrived on the scene as a new diagnostic tool for primary lesions.

In this chapter, we describe the present status of radiologic diagnosis of gastric carcinoma using CCD-DR at our center, report our experience of MDCT gastrography in the preoperative staging of gastric carcinoma, and discuss the future prospects for radiographic diagnosis of gastric carcinoma using these new diagnostic techniques.

Advanced Digital Radiographic Systems for Gastric Diagnosis

In our hospital, images yielded by radiography of the gastrointestinal tract became completely digitalized with the adoption of CCD-DR (DR-2000H; Hitachi Medical, Tokyo, Japan) in 1999. At present, hard copies of diagnostic images are prepared for interpretation, but monitor-based diagnosis is yet to become a reality. Our radiographic investigations of the gastrointestinal tract use three CCD-DR systems: one C-arm type, one over-tube type, and one under-tube type. Each CCD-DR is connected by a DR network to two laser printers and an image server, and in parallel with the scanning procedure, reference images are forwarded to the hospital information system via a gateway after DICOM (digital imaging and communication in medicine) conversion at the same time as the diagnostic images are processed. After DICOM

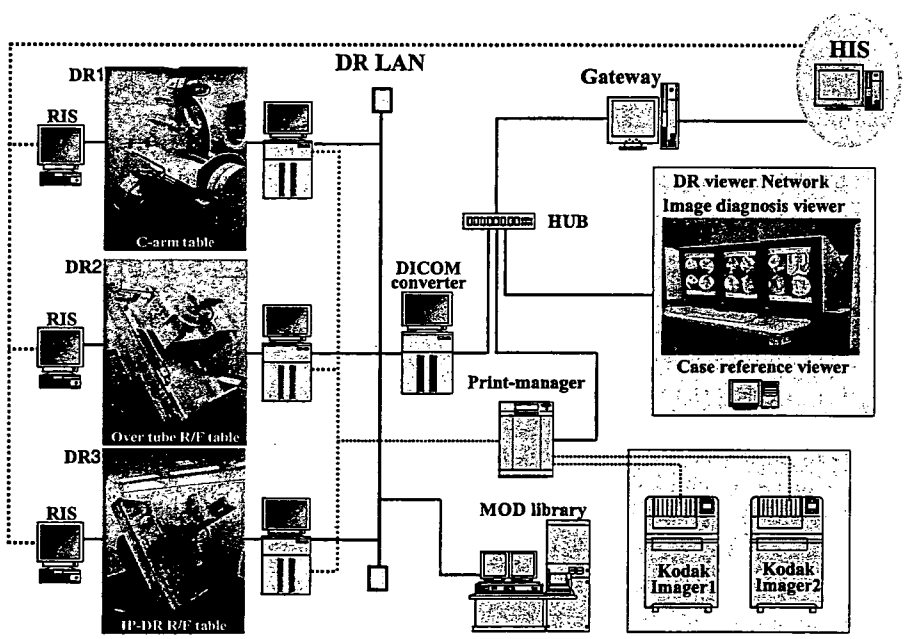

FIG. 1. Advanced digital radiography system for gastric diagnosis. Three charge-coupled device-digital radiography (CCD-DR) units are routinely used for gastric examinations in our hospital. Each unit connects with a DR network, and the images can be diagnosed on an image workstation

conversion, the images are accessible for monitor diagnosis at an image workstation with three viewers (Fig. 1).

The Status of CCD-DR-Based Radiographic Examination of Gastric Carcinoma

At our center, we use 250–300 ml barium at a 130–140 w/v% concentration in gastric radiographic studies. The scanning methods employed are the filling method, double-contrast radiography, and the compression method, but the core diagnostic technique in radiographic diagnosis of gastric carcinoma is double-contrast imaging obtained with barium (positive contrast medium) and gas (negative contrast medium). After barium is swallowed, the patient is given 5 g of a foaming agent, and by distending the stomach via the CO_2 gas so produced, we are able to easily obtain double-contrast images. The barium contained in the gas-distended stomach moves with changes in posture, and double-contrast images of excellent quality are obtained by ensuring that the barium adheres uniformly to the mucosal surfaces. Unlike the filling and compression methods, double-contrast imaging is indispensable for the visualization of early gastric carcinoma, which is characterized by few irregularities of the mucosal surfaces (Fig. 2). With gastric radiography based on the double-contrast method, we can easily identify the macroscopic types of gastric carcinomas, their exact extensions and locations in the stomach (Figs. 3–6). However, viewing double-contrast images obtained with contrast provided by gas and barium requires a broad dynamic range. The dynamic range for CCD-DR images adequately covers the image quality required for gastric radiography, and the image quality matches that in conventional FSS. Additionally, CCD-DR digital images also enable the optimization of image quality via image processing after scanning and, compared with FSS, are relatively well matched image by image and allow standardized diagnostic images to be obtained.

Comparative Evaluation of FSS and CCD-DR in the Diagnosis of Gastric Carcinoma

We conducted a prospective study to evaluate the difference in diagnostic accuracy between FSS and CCD-DR, and reported in a publication of *Radiology* [8]. From January to February 1997, we randomly assigned patients scheduled for gastric radiography to either FSS or CCD-DR; 112 patients were examined by FSS and 113 by CCD-DR. Six radiologists who were blinded to the clinical details assessed the films for each patient with a six-level confidence rating for the presence or absence of gastric carcinoma. The CCD-DR images in this study were prepared as hard copies for diagnosis. The diagnoses for each patient were rated against those produced by three other radiologists who conducted the actual radiographic examinations and were aware of all clinical data, such as endoscopic findings and the pathology of biopsy specimens. The sensitivity and specificity of FSS and CCD-DR for gastric carcinoma were determined from the assessments obtained, the difference between the two modalities was statistically analyzed, and a comparison was performed by receiver-operating characteristic (ROC) analysis. The study yielded a diagnosis of gastric carcinoma by FSS in 24 patients and by CCD-DR in 27 patients; the sensitivity for diagnosing the presence of gastric carcinoma was 64.6% and 75.3%, respectively

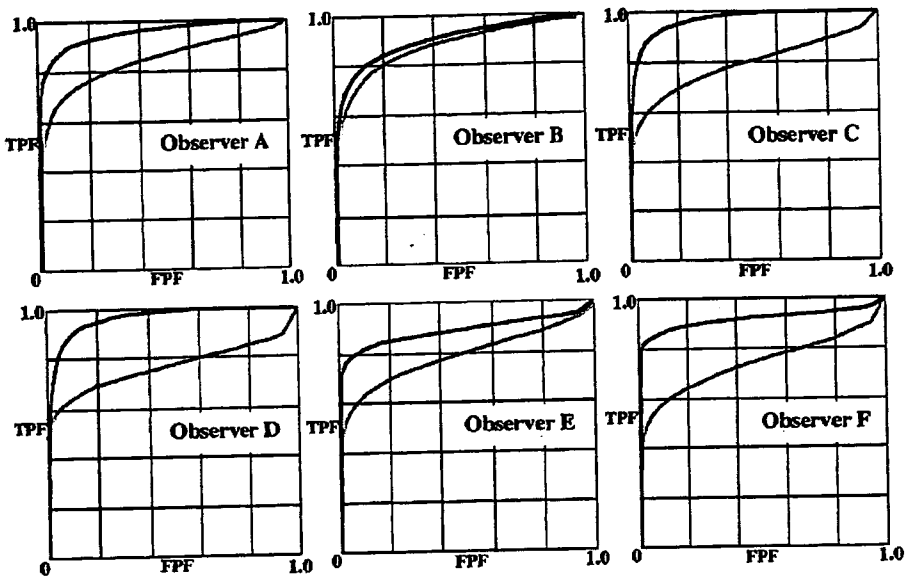

FIG. 7. Receiver operating characteristic (ROC) curves obtained from six observers. All observers achieved more accurate results with CCD-DR than with conventional radiography. Diagnostic accuracy of CCD-DR is clearly superior to that of conventional radiography. (Used with permission from Radiological Society of North America)

($P = 0.278$), and the specificity was 84.5% and 90.5%, respectively ($P = 0.011$). The ROC analysis [11] also showed that the diagnostic performance of CCD-DR was clearly superior (Fig. 7).

Usefulness of Radiography of Gastric Carcinoma by CCD-DR

The diagnostic performance of CCD-DR for gastric carcinoma is adequately comparable to that of FSS, indicating that the digitalization of images in gastric radiography is entirely feasible. The future adoption of diagnosis by monitor display will make possible the real-time display and optimization of diagnostic images and enable greater ease of image storage and retrieval. Capitalizing on these advantages of digitalization promises to yield an efficient and effective diagnostic environment for screening and preoperative staging, as compared with the conventional FSS modality.

Preoperative Evaluation of Gastric Carcinoma Using MDCT

To date, the role of radiographic CT studies in the preoperative staging of gastric carcinoma has primarily involved evaluating invasion of surrounding organs or metastasis to lymph nodes or other organs, and it was rare for it to be used for evaluation of the primary tumor itself [12,13]. However, the advent of MDCT has made possible the arrival of full-scale volume scans, facilitating high-speed, detailed image acquisition over an extensive area. The degree of resolution of CT images has improved

dramatically with MDCT, enabling the detailed evaluation of local lesions and the detection of small metastases, even in ordinary axial images [14]. Moreover, workstations that are capable of processing the massive quantities of image data produced by MDCT have been developed, and the three-dimensional CT visualization of gastric lesions, which is called MDCT gastrography, has become straightforward. This trend is fairly flourishing in the diagnosis of colorectal cancer as MDCT colonography, which is considered to have a great potential of being a modality for colorectal cancer screening [15–17].

Three-Dimensional Visualization of the Stomach by MDCT Gastrography

To visualize gastric lesions in three dimensions using MDCT, it is necessary to distend the gastric lumen with a foaming agent (CO_2 gas). As a consequence of the contrast between the gas and the inner gastric surface, owing to the substantial difference in density, it is possible to effortlessly prepare 3D images of the inner gastric surface. MDCT gastrography employs two methods for visualization, virtual endoscopic views and 3D gas insufflation views, obtained by 3D processing of the CT image data (Fig. 8).

Evaluation of the Detectability of Gastric Carcinoma by MDCT Gastrography

In the 3-month period between March and June 2003, we evaluated 4-row MDCT (Aquilion; Toshiba Medical Systems, Tokyo, Japan) in 84 gastric carcinoma patients who underwent MDCT for preoperative staging. Each scan was performed with the standard abdominal scan parameter settings for preoperative staging using automatic exposure control [18]. We prepared virtual endoscopic and 3D gas insufflation views from the image data obtained for each patient by MDCT volume scans, and two radiologists prepared responses on the basis of all clinical data for each patient, including gastroscopic findings, and the detectability of gastric carcinoma was evaluated by consensus for each display method. Eighty-six gastric carcinoma lesions (44 early and 42 advanced lesions) were diagnosed in the 84 patients. The detectability by virtual endoscopic and 3D gas insufflation views by MDCT gastrography was 47.7% and 40.9%, respectively, for early lesions (Table 1), and 59.5% and 76.2% for advanced lesions (Table 2). Hence, the detectability was less than 50% for early lesions, but about 60%–70% for advanced lesions of gastric carcinoma [19]. Especially in early lesions, all protruded-type lesions could be recognized, while less than half of depressed-type lesions, which is a common type of early gastric carcinoma, were missed (Figs. 9, 10).

TABLE 1. Detectability for 44 early gastric carcinomas by multidetector row computed tomography (MDCT) gastrography

	Protruded type	Flat elevated type	Depressed type	Total
Virtual endoscopic views	100% (2/2)	50.0% (1/2)	45.0% (18/40)	47.7% (21/44)
Three-dimensional gas insufflation views	100% (2/2)	50.0% (1/2)	37.5% (15/40)	40.9% (18/44)

TABLE 2. Detectability for 42 advanced gastric cancers by MDCT gastrography

	Borrman I type	Borrman II type	Borrman III type	Borrman IV type	Total
Virtual endoscopic view	0% (0/1)	84.6% (11/13)	68.8% (11/16)	25.0% (3/12)	59.5% (25/42)
Three-dimensional gas insufflation view	0% (0/1)	76.9% (10/13)	68.8% (11/16)	91.7% (11/12)	76.2% (32/42)

MDCT gastrography is presently inadequate for the detection of gastric carcinoma and its potential for clinical application is low.

Potential for MDCT Gastrography in Preoperative Staging for Gastric Carcinoma

MDCT gastrography is simpler and less invasive than endoscopy and radiography, and permits evaluation of the stomach overall in an examination of short duration. Detection of early lesions is challenging, and although it therefore has low potential as a screening method, it is capable of detecting lesions that are advanced to a certain extent, and also of simultaneously detecting lesions in other organs of the abdomen. In preoperative staging, as for radiography, it is capable of objectively ascertaining the position and overall picture of the primary lesion, and of diagnosing the relations between the degree of extramural invasion and surrounding organs. With the axial images of MDCT, representing a quantum leap in resolution compared with normal CT, it was possible to also diagnose correctly lymph node metastasis. Because MDCT itself is an examination method required for the preoperative diagnosis of local spread or remote metastasis of gastric carcinoma, it is highly likely at present that it can partially replace the role of radiography or ultrasound endoscopy. As well, because the image data of MDCT is digitalized density information, it is possible to selectively visualize 3D information in a manner that is effective for diagnosis, and has a great potential of being a modality for computer-aided diagnosis [20]. By digitally combining the 3D view of the primary lesion and the 3D image data of diagnosed lymph node metastasis, it will be possible to provide surgeons with effective preoperative 3D views of gastric carcinoma (Fig. 11).

Conclusions

As a result of future advancements in image engineering and computer technology, digital radiographic systems and MDCT systems will continue to evolve, and it can be predicted that new diagnostic methods that utilize the advantages of digitalization in the radiological diagnosis of gastric carcinoma will also be developed. MDCT gastrography has little potential at present as a diagnostic method for the primary lesions of gastric carcinoma. However, with further advances in MDCT, higher-speed examinations, improved image quality, and optimization of exposure dose, it appears certain that MDCT gastrography will gradually replace radiography, endoscopy, and ultrasound endoscopy.

Acknowledgments. This work was supported by Grants for Scientific Research Expenses for Health and Welfare Programs and the Foundation for the Promotion of Cancer Research, and by the 3rd-term Comprehensive 10-year Strategy for Cancer Control from the Ministry of Health, Labor and Welfare.

References

1. Templeton FE (1964) X-ray examination of the stomach, rev edn. University of Chicago Press, Chicago
2. Kuru M (1966) X-ray diagnosis. In: Atlas of early gastric carcinoma of the stomach. Nakayama-Shoten, Tokyo, pp 219–223
3. Shirakabe H, Ichikwa H, Kumakura K, et al (1966) Atlas of X-ray diagnosis of early gastric cancer. Igaku Shoin, Tokyo
4. Ichikawa H (1993) X-ray diagnosis of early gastric cancer. Gastric cancer. Springer-Verlag, Tokyo, pp 232–245
5. Okumura T, Maruyama M (1993) A prospective study on advanced gastric cancer detection by mass screening. Gastric Cancer. Springer-Verlag, Tokyo, pp 263–277
6. Sonoda M, Takano M, Miyahara J, et al (1983) Computed radiography utilizing scanning laser stimulated luminescence. Radiology 148:833–838
7. Hillman BJ, Ovitt TW, Nudelman S, et al (1981) Digital video subtraction angiography of renal vascular abnormalities. Radiology 139:277–280
8. Iinuma G, Ushio K, Ishikawa T, et al (2001) Diagnosis of gastric cancers: comparison of conventional radiography with a 4 million-pixels charge-coupled device. Radiology 214: 497–502
9. Berland LL, Smith JK (1998) Multidetector-array CT: once again, technology creates new opportunities. Radiology 209:327–329
10. Hu H, He HD, Foley WD, Fox SH (2000) Four multidetector-row helical CT: image quality and volume coverage speed. Radiology 215:55–62
11. Metz CE, Goodenough DJ, Rossmann K (1973) Evaluation of receiver operating characteristic curve data in terms of information theory, with applications in radiography. Radiology 109:297–303
12. Botet JF, Lightdale CJ, Zauber AG, et al (1991) Preoperative staging of gastric cancer: comparison of endoscopic US and dynamic CT. Radiology 181:426–432
13. Habermann RC, Weiss F, Riecken R, et al (2004) Preoperative staging of gastric adenocarcinoma: comparison of helical CT and endoscopic US. Radiology 230:465–471
14. Ba-Ssalamah A, Prokop M, Uffmann M, et al (2003) Dedicated multidetector CT of the stomach: spectrum of diseases. *Radiographics* 181:426–432
15. Dachman A (2003) Atlas of virtual colonoscopy. Springer-Verlag, New York
16. Iannaccone R, Laghi A, Catalano C, et al (2003) Detection of colorectal lesions: lower-dose multi-detector row helical CT colonography compared with conventional colonoscopy. Radiology 229:775–781
17. Macari M, Bini EJ, Jacobs SL, et al (2004) Colorectal polyps and cancers in asymptomatic average-risk patients: evaluation with CT colonography. Radiology 230:629–636
18. Itoh S, Ikeda M, Mori Y, et al (2002) Lung: feasibility of a method for changing tube current during low-dose helical CT. Radiology 224:905–912
19. Iinuma G, Moriyama N (2004) Clinical potential of CT gastrography for visualization of gastric cancers. In: Recent advances in gastric cancers: the 17th International Symposium of Foundation for Promotion of Cancer Research, pp 37–38
20. Summers RM (2003) Road maps for advancement of radiologic computer-aided detection in the 21st century. *Radiology* 229:11–13

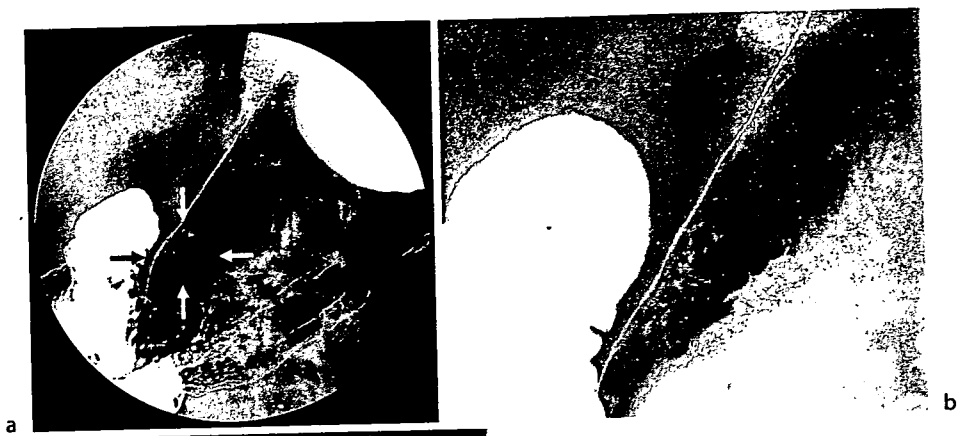

a b

c

FIG. 2. A 55-year-old man. A flat lesion is visualized at the lesser curvature side of the lower gastric body (a, *arrows*). CCD-DR clearly delineates the irregular surface of the lesion (b). Gross specimen shows a flat type of early gastric cancer, 2.5 × 1.5 cm in size (c)

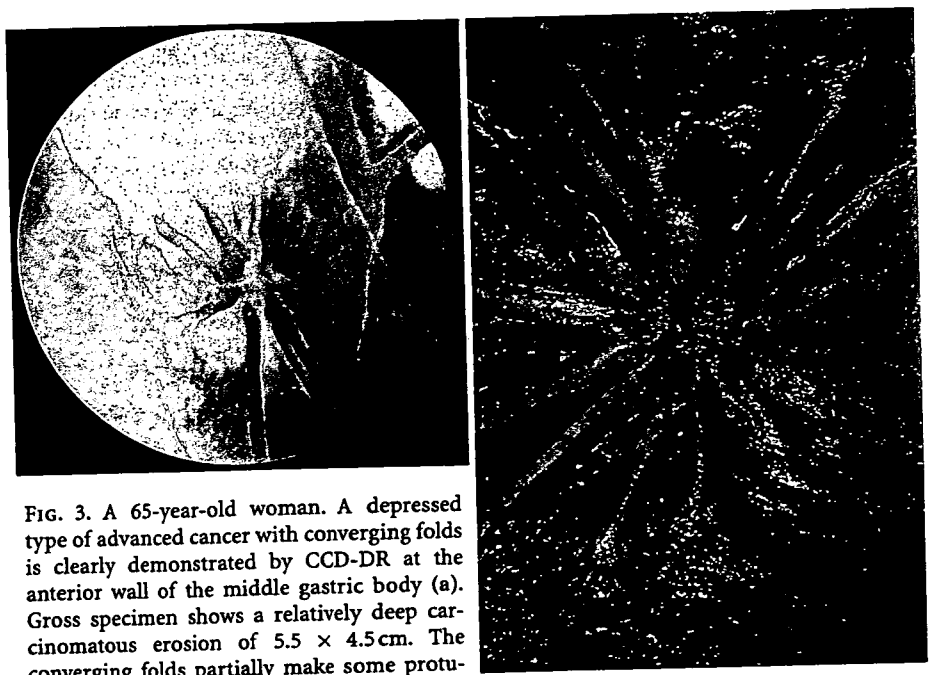

a b

FIG. 3. A 65-year-old woman. A depressed type of advanced cancer with converging folds is clearly demonstrated by CCD-DR at the anterior wall of the middle gastric body (a). Gross specimen shows a relatively deep carcinomatous erosion of 5.5 × 4.5 cm. The converging folds partially make some protuberance at the margin of the lesion (b)

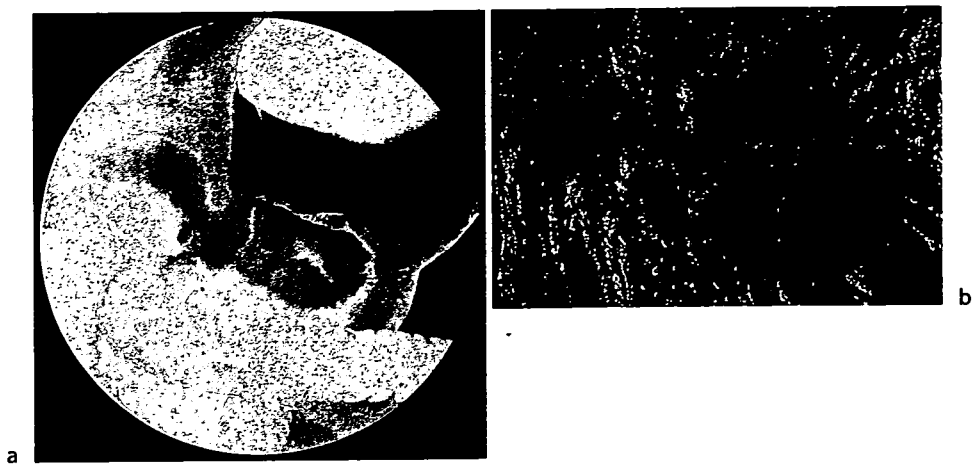

a b

FIG. 4. A 70-year-old man. CCD-DR visualizes two gastric cancers at the posterior of the lower gastric body to the antrum (a). Gross specimen demonstrates a protruded advanced cancer with central ulceration measuring 4.0 cm and a protruded type of early cancer measuring 2.0 cm (b)

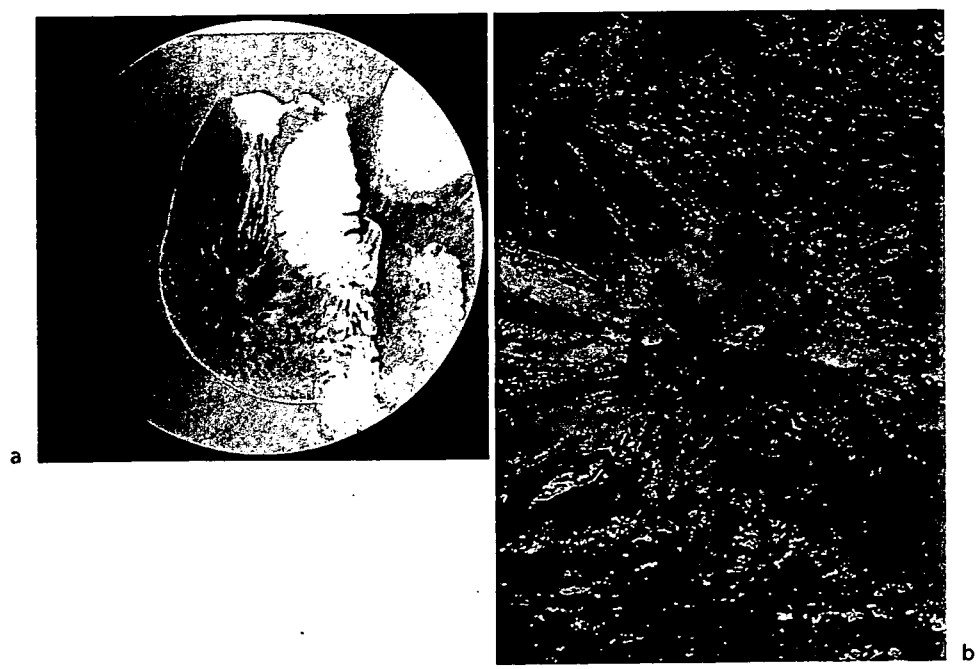

a b

FIG. 5. A 55-year-old man. CCD-DR demonstrates a depressed type of gastric cancer at the posterior wall of the antrum (a). Gross specimen shows a depressed type of advanced cancer 5.0 × 4.5 cm in size (b)

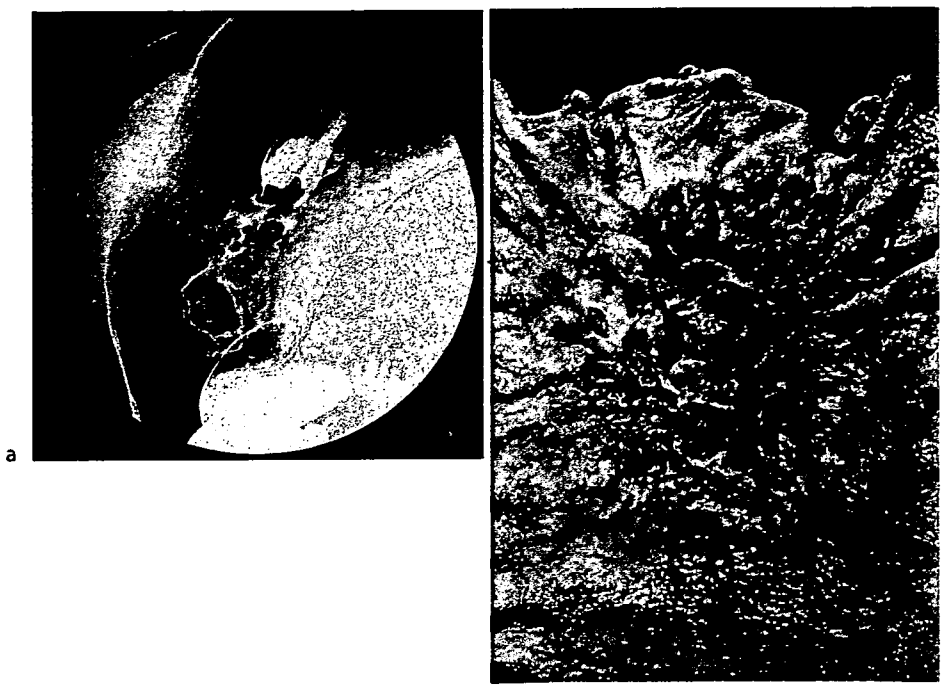

a b

FIG. 6. A 71-year-old man. An advanced cancer is demonstrated by CCD-DR just below the cardia (a). Gross specimen shows an ulcerative type of advanced gastric cancer 6.0 cm in diameter (b)

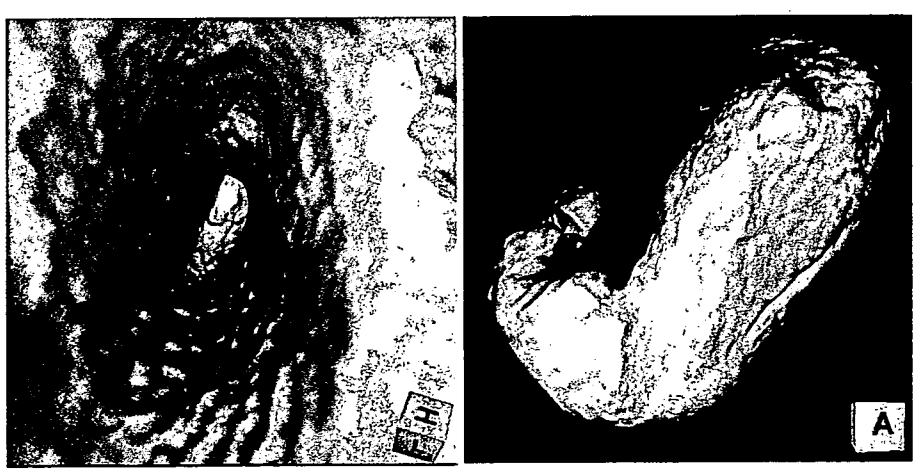

a b

FIG. 8. Two imaging modes of multidetector row computed tomography (MDCT) gastrography. a A representative virtual endoscopic view, resembling gastroscopic images. b A representative 3D gas insufflation view, resembling radiographic images

FIG. 9. A 63-year-old man. Conventional endoscopy demonstrates a protruded type of early gastric cancer 2 cm in size at the greater curvature side of the upper gastric body (a). The lesion is clearly visualized by virtual endoscopic view (b)

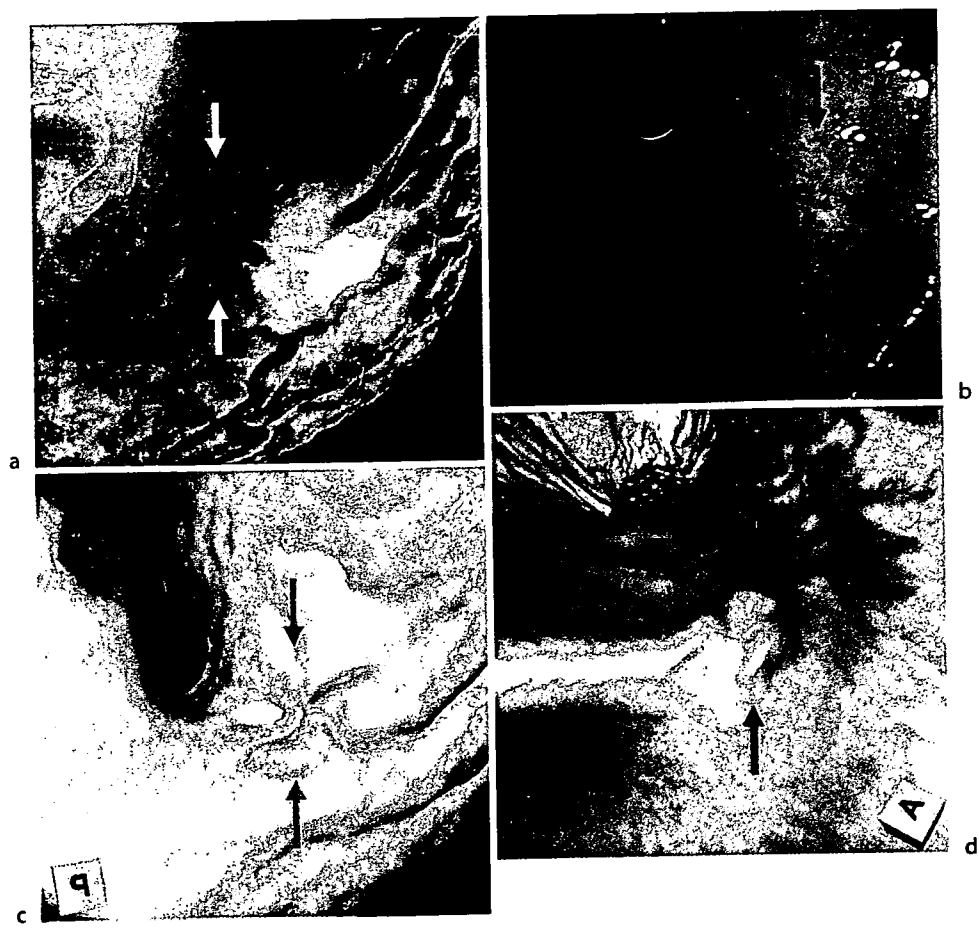

FIG. 10. A 33-year-old man. A small depressed type of early gastric cancer measuring 1.5 cm is identified at the posterior side of the gastric angle by gastric radiography and gastroscopy (*arrows* in a, b). The lesion can barely be recognized by virtual endoscopic and 3D views of MDCT gastrography (*arrows* in c, d)

FIG. 11. Three-dimensional imaging of a gastric cancer and lymph node metastases. The 3D view of the primary lesion (*arrow*) and the 3D image data of diagnosed lymph node metastases can be combined digitally to produce effective 3D views of gastric carcinoma in the pre-operative staging